NASA/TM—2004-213045

Performance of Thermal Mass Flow Meters in a Variable Gravitational Environment

John E. Brooker and Gary A. Ruff
Glenn Research Center, Cleveland, Ohio

April 2004

The NASA STI Program Office . . . in Profile

Since its founding, NASA has been dedicated to the advancement of aeronautics and space science. The NASA Scientific and Technical Information (STI) Program Office plays a key part in helping NASA maintain this important role.

The NASA STI Program Office is operated by Langley Research Center, the Lead Center for NASA's scientific and technical information. The NASA STI Program Office provides access to the NASA STI Database, the largest collection of aeronautical and space science STI in the world. The Program Office is also NASA's institutional mechanism for disseminating the results of its research and development activities. These results are published by NASA in the NASA STI Report Series, which includes the following report types:

- TECHNICAL PUBLICATION. Reports of completed research or a major significant phase of research that present the results of NASA programs and include extensive data or theoretical analysis. Includes compilations of significant scientific and technical data and information deemed to be of continuing reference value. NASA's counterpart of peer-reviewed formal professional papers but has less stringent limitations on manuscript length and extent of graphic presentations.

- TECHNICAL MEMORANDUM. Scientific and technical findings that are preliminary or of specialized interest, e.g., quick release reports, working papers, and bibliographies that contain minimal annotation. Does not contain extensive analysis.

- CONTRACTOR REPORT. Scientific and technical findings by NASA-sponsored contractors and grantees.

- CONFERENCE PUBLICATION. Collected papers from scientific and technical conferences, symposia, seminars, or other meetings sponsored or cosponsored by NASA.

- SPECIAL PUBLICATION. Scientific, technical, or historical information from NASA programs, projects, and missions, often concerned with subjects having substantial public interest.

- TECHNICAL TRANSLATION. English-language translations of foreign scientific and technical material pertinent to NASA's mission.

Specialized services that complement the STI Program Office's diverse offerings include creating custom thesauri, building customized databases, organizing and publishing research results . . . even providing videos.

For more information about the NASA STI Program Office, see the following:

- Access the NASA STI Program Home Page at ***http://www.sti.nasa.gov***

- E-mail your question via the Internet to help@sti.nasa.gov

- Fax your question to the NASA Access Help Desk at 301–621–0134

- Telephone the NASA Access Help Desk at 301–621–0390

- Write to:
  NASA Access Help Desk
  NASA Center for AeroSpace Information
  7121 Standard Drive
  Hanover, MD 21076

NASA/TM—2004-213045

Performance of Thermal Mass Flow Meters in a Variable Gravitational Environment

John E. Brooker and Gary A. Ruff
Glenn Research Center, Cleveland, Ohio

National Aeronautics and
Space Administration

Glenn Research Center

April 2004

Acknowledgments

The authors would like to acknowledge the assistance of those individuals who aided in the preparation of this document. Eric Neumann (Facilities and Test Engineering Division), Jack Kolis (Test Installations Division), and Joe Wilson (Test Installations Division) for mechanical design, fabrication, and assembly of the experiment hardware and also Jim Withrow (Facilities and Test Engineering Division) for electrical design and conducting the experiment on the KC-135. Jack Weigand (Logistics and Technical Information Division) for assistance in estimating uncertainties associated with calibration equipment. This report documents the performance of five thermal mass flow meters from four different manufacturers. It should be noted that a single meter from each lot was used to collect the data and does not represent the performance of the entire meter population.

Available from

NASA Center for Aerospace Information
7121 Standard Drive
Hanover, MD 21076

National Technical Information Service
5285 Port Royal Road
Springfield, VA 22100

Available electronically at http://gltrs.grc.nasa.gov

Performance of Thermal Mass Flow Meters in a Variable Gravitational Environment

John E. Brooker and Gary A. Ruff
National Aeronautics and Space Administration
Glenn Research Center
Cleveland, Ohio 44135

The performance of five thermal mass flow meters, MKS Instruments 179A and 258C, Unit Instruments UFM-8100, Sierra Instruments 830L, and Hastings Instruments HFM-200, were tested on the KC-135 Reduced Gravity Aircraft in orthogonal, coparallel, and counterparallel orientations relative to gravity. Data was taken throughout the parabolic trajectory where the g-level varied from 0.01 to 1.8 times normal gravity. Each meter was calibrated in normal gravity in the orthogonal position prior to flight followed by ground testing at seven different flow conditions to establish a baseline operation. During the tests, the actual flow rate was measured independently using choked-flow orifices. Gravitational acceleration and attitude had a unique effect on the performance of each meter. All meters operated within acceptable limits at all gravity levels in the calibrated orthogonal position. However, when operated in other orientations, the deviations from the reference flow became substantial for several of the flow meters. Data analysis indicated that the greatest source of error was the effect of orientation, followed by the gravity level. This work emphasized that when operating thermal flow meters in a variable gravity environment, it is critical to orient the meter in the same direction relative to gravity in which it was calibrated. Unfortunately, there was no test in normal gravity that could predict the performance of a meter in reduced gravity. When operating in reduced gravity, all meters indicated within ±5% of the full scale reading at all flow conditions and orientations.

INTRODUCTION

Thermal mass flow meters (MFM) and controllers are commonly used in industry, laboratories, and recently in space flight experiments such as Combustion Module-1, which first flew in 1997 aboard the space shuttle Columbia. These applications depend upon accurate fluid flow measurements to provide necessary information for process control, fluid delivery, and subsequent data analysis. In a terrestrial environment, a properly installed and calibrated device should be adequate for most applications. However, in an environment where the gravitational level is reduced or variable, special precautions should be taken to ensure proper delivery of gases. (Why these flow meters may be particularly susceptible to gravitational effects will be identified in a later section when discussing the theory of operation.) The purpose of this research is to determine the effect of gravitational acceleration on the performance of five thermal MFMs from four manufacturers[1] as identified in Table 1. These meters were selected for evaluation because they are representative of those used in the Microgravity Science Division at NASA GRC, not because they are representative of all commercially-available flow meters. No endorsement for use of these meters is implied. This study is intended to give the reader information on the application of thermal MFMs and provide those that have used these types of instruments an example of potential systematic errors that may exist through off-nominal use.

Table 1. Mass Flow Meters and Manufacturers

Manufacturer	Model	Designation
MKS Instruments	179A	MKS179A
MKS Instruments	258C	MKS258C
Unit Instruments	UFM-8100	UFM8100
Sierra Instruments	830L	SI830L
Hastings Instruments	HFM-200	HFM200

THEORY OF OPERATION

HFM200

As reported by the manufacturer [1], the Hastings HFM-200 series instrument operates on a thermal electric principle whereby flow through a metallic capillary tube, which is a fixed percentage of the total flow through the instrument, is heated uniformly by a resistance winding attached to the midpoint of the capillary. Two thermocouples are welded at equal distances from the midpoint and develop equal outputs at zero flow. When flow occurs through the tubing, heat is transferred from the tube to the gas on the inlet side,

[1] Only one mass flow meter from each lot was tested, therefore the results do not represent the entire meter population.

and from the gas back to the tube on the outlet side creating an asymmetrical temperature distribution. The thermocouples sense the change in capillary tube temperature and produce approximately a 1 millivolt full scale output signal proportional to that change. This signal is amplified by the meter circuitry to provide a 0-5 VDC output. For a constant power input, the differential thermocouple output is a function of the mass flow rate and the heat capacity of the gas. Since the heat capacity of many gases is relatively constant over wide ranges of temperature and pressure, the flow meter may be calibrated directly in mass units for those gases. The HFM200 sensor measures approximately 10 sccm full scale flow. Measurement of flow rates higher than the 10 sccm full scale is achieved by dividing the flow with a fixed ratio shunting arrangement. This is accomplished by placing the measuring capillary tube in parallel with a laminar flow element that generates a pressure drop proportional to the mass flow rate. Therefore, the sensor only needs to heat the gas passing through the capillary tube.

MKS179A, MKS258C, UFM8100, SI830L

The theory of operation for the MKS179A, MKS258C, UFM8100, and SI830L is basically the same as described above with several exceptions [2]. At the midpoint of the capillary tube, two wire coils are wrapped side by side. The windings serve as both heaters and temperature sensors. The MFM electronics provide a constant current to the coils which are heated by the resistance of the wire. Since the resistance of the coils varies with temperature, the coils function as resistance temperature detectors which respond to changes in the gas temperature. Each coil is part of a resistive leg in a Wheatstone bridge circuit. When there is no gas flow, heat from the coils generates a uniform temperature gradient about the midpoint of the tube. When gas flows through the sensor, the upstream coil will cool as heat is transferred to the gas. At the downstream coil, the gas temperature is higher so the downstream coil cools only slightly. Assuming all other heat losses for the coils are the same, the temperature difference between the coils can be linearly correlated to the mass flow rate. The electronics in the MFM convert the temperature difference to a 0-5 VDC output. While the MKS179A, MKS258C, UFM8100, and SI830L instruments operate on the same principle, there are differences in the construction and circuitry that could affect their behavior in a variable gravity environment.

Gravitational Effects

Any instrument in which heat transfer is essential to obtain a measurement could be affected by variations in the magnitude or direction of the gravity vector. Tison [3] performed a detailed investigation of the performance of thermal flow meters and quantified the errors in the zero and span readings associated with the use of gas correction factors, meter orientation, and variations of upstream pressure and temperature. In this work, he found that the orientation of the meter in normal gravity changed the zero indication by less than 0.44% of full scale and the effect on the span was negligible. Of course, all of tests were conducted in normal gravity so only the direction of the gravity vector was varied. Kondo *et al*. [4] and Weinheimer and Ridley [5] have investigated the effect of ambient pressure on thermal mall flow controllers and measured flow errors of factors of 2 to 3 when the pressure is reduced to a few millibars. These errors became significant only when the ambient pressure was reduced below about 50 mbar. Furthermore, Weinhiemer and Ridley [5] found that the sign of the error was reversed for flow meters from different manufacturers and depended on their specific design and operating characteristics. They concluded that variations in the heat transport involving the air near the sensing thermistors played a role in these errors.

Given that thermal mass flow meters respond to any external stimuli that alter the heat transfer within the device, it is likely that variations in both the magnitude and direction of the gravity vector could also produce errors in the flow measurement. Because of the small diameter of the capillary tube, buoyancy plays a negligible role on the fluid flowing through the tube. [3] However, all the instruments operate by heating a portion of the capillary tube. A change in the natural convection from the outside of the capillary tube by a change in the gravity level or orientation of the meter would be interpreted by the instrument as a change in the flow, resulting in an inaccurate measurement. This effect may be alleviated by judiciously insulating the tube but the specific type and placement of the insulation could produce varying performance, even between otherwise identical instruments. Other structural differences, such as how the heating wires are bonded to the capillary, could also introduce an effect of either gravity or orientation. The purpose of this study is to quantify these effects. A detailed evaluation of the design of each MFM to determine why they perform the way they do was beyond the scope of this investigation. As previously stated, no endorsement of any flow meter or manufacturer is implied by NASA or the authors.

HARDWARE DESCRIPTION

The experiment package consisted of a test platform, a gas delivery system, and a data acquisition and control (DAC) system. On the test platform, all five mass flow meters were oriented in the same direction and secured to a plate. A critical flow orifice was installed upstream of each meter. The orifice provided a non-thermal flow

measurement with which the results could be compared. The platform could be positioned in different flow orientations relative to the gravity vector as depicted in Figure 1. A three-axis accelerometer was mounted on the plate to provide measurements of local acceleration.

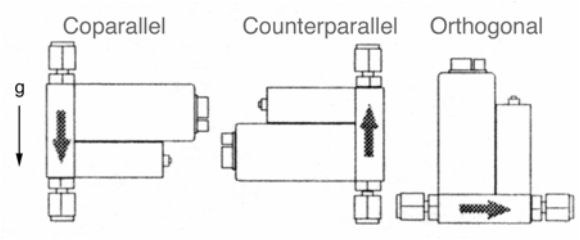

Figure 1. MFM position relative to gravity vector

The gas delivery system contained a gas bottle (Air Products UHP Zero Grade Air) and various components to provide the test devices with a smooth and continuous supply of air. A flow schematic is shown in Appendix A. Data acquisition and control was performed by a PC-based measurement system as described below.

The transducers used for this experiment included five MFMs, two pressure sensors (ambient and gas), two K-type thermocouples (ambient and gas), and a three-axis accelerometer producing a total of 12 analog signals. A portable, modular signal conditioning system (National Instruments SCC-2345) containing a thermocouple input module and five lowpass filter modules was used in conjunction with a multifunction I/O card (National Instruments DAQCard-AI-16XE-50) with 16-bit resolution and 20 kHz sampling rate for signal measurement and conditioning. National Instruments LabVIEW Version 5 was used as the application software on a Dell D266XT notebook computer with Microsoft NT 4.0 as the operating system. Data was collected at 100 Hz sampling rate per channel.

PROCEDURE

Prior to testing, each instrument used in this experiment was calibrated by the NASA GRC Calibration. Appendix B summarizes the first-order linear regression models for each instrument used in this experiment. All mass flow meters were calibrated only in the orthogonal attitude in order to evaluate its performance in an off-nominal orientation, i.e., using the meter in an orientation different than the calibration procedure. Orifice flow rates were calculated from a first-order linear regression model also supplied by the Calibration Lab. Ground-based experiments were performed prior to flight to a baseline performance at normal gravity. Data was collected throughout the entire flight maneuver encompassing a variable gravitational environment between 0.01 and 1.8 times normal gravity. The analysis was performed on data sampled at one second increments from a ten second time interval in each of the three gravity regimes (normal, reduced, and elevated).

DATA REDUCTION

The data set consisted of three independent variables: inlet gas pressure (7 levels), gravity level (3 levels), and orientation (3 levels), with one dependent variable, flow rate. MFM performance was measured by calculating the difference between orifice and meter flow rate using the equation

$$D_{mfm} \equiv \left(F_{orf} - F_{mfm}\right) \tag{1}$$

where D_{mfm} is the meter departure function and F_{orf} and F_{mfm} are the flow rate measured by the orifice and thermal flow meter, respectively. Therefore, a departure function could be determined as a function of inlet gas pressure for each meter at any gravity level and orientation. These results will be discussed later after the experimental uncertainties associated with this experiment have been addressed.

UNCERTAINTY ANALYSIS

The performance of the thermal flow meters in a variable-g environment can only be quantified relative to the uncertainty existing in the measurement. The analysis of uncertainties in experimental measurements and calculations applied in this study was consistent with the methods outlined in the ANSI/ASME Standard PTC 19.1[6] and conducted according to the procedures formulated in Coleman and Steele [7]. A brief summary of the method applied in this work is provided below.

Propagation of Systematic Uncertainties into Experimental Result

Each value of an individual variable that is measured contains elemental error sources in the form of systematic and random errors. These errors propagate into the data reduction equation as shown in Fig. 2, and yield the systematic and random uncertainties of the experimental result. The general data reduction equation is given by

$$r = r\left(X_1, X_2, ..., X_J\right) \tag{2}$$

where r is the experimental result and X_J is a measured variable. The systematic uncertainties from elemental error sources must be estimated and combined to form the estimate of the systematic uncertainty for each measured variable. The root-sum-square combination of M elemental errors sources for measured variable J is

$$B_J^2 = \sum_{k=1}^{M} (B_J)_k^2 \tag{3}$$

where B_J is the systematic uncertainty and $(B_J)_k$ is the uncertainty from an elemental error source. These systematic uncertainties propagate into the data reduction equation as described by

$$B_r^2 = \sum_{i=1}^{J} \left(\frac{\partial r}{\partial X_i} \right)^2 B_i^2 + 2 \sum_{i=1}^{J-1} \sum_{k=i+1}^{J} \left(\frac{\partial r}{\partial X_i} \right) \left(\frac{\partial r}{\partial X_k} \right) B_{ik} \tag{4}$$

where B_r is the systematic uncertainty for the result, B_i is the systematic uncertainty of measured variable X_i, and B_{ik} is the covariance estimator accounting for correlated systematic uncertainties between measured variables (variables that share the same elemental error sources). A satisfactory approximation for the correlated systematic uncertainty is

$$B_{ik} = \sum_{\alpha=1}^{L} (B_i)_\alpha (B_k)_\alpha \tag{5}$$

where L is the number of elemental systematic error sources that are common for measurements of variables X_i and X_k.

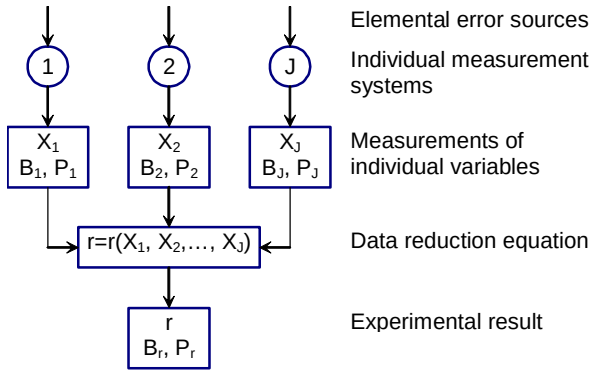

Figure 2. Propagation of errors into experimental results [7]

Random Uncertainty of Experimental Result: Multiple Tests Method

Calculating the random uncertainty associated with a data reduction equation is best accomplished from direct determination using multiple tests. For a single test replicated M times, the mean value of the result is

$$\bar{r} = \frac{1}{M} \sum_{k=1}^{M} r_k \tag{6}$$

where r_k is the measured result from a single test. The standard deviation of the sample population of the M individual tests is given by

$$S_r^2 = \frac{1}{M-1} \sum_{k=1}^{M} (r_k - \bar{r})^2 \tag{7}$$

and the standard deviation of the average result from the M individual tests is

$$S_{\bar{r}} = \frac{S_r}{\sqrt{M}} \tag{8}$$

From these equations, the random uncertainty of the mean result for $M \geq 10$ is calculated using

$$P_{\bar{r}} = t S_{\bar{r}} \tag{9}$$

where the value of t is taken from a t-distribution table at the 95% confidence interval. The systematic uncertainty associated with the mean result from Eq. (6) is the same as that found for a single test since systematic errors are fixed and not affected by averaging the results of multiple tests. Therefore, the total uncertainty in the mean result at the 95% confidence level is expressed as

$$U_{\bar{r}}^2 = B_r^2 + P_{\bar{r}}^2 \tag{10}$$

First-Order Linear Regression Uncertainty

When experimental results are represented by a regression model, the uncertainty associated with the original data will propagate into the values that are predicted by the model. For this analysis, a first-order linear model was utilized. By the method of least squares, the coefficients of the first-order model generated from N data pairs of (X_i,Y_i) are

$$a_0 = \frac{\sum_{i=1}^{N} X_i^2 \sum_{i=1}^{N} Y_i - \sum_{i=1}^{N} X_i \sum_{i=1}^{N} X_i Y_i}{N \sum_{i=1}^{N} X_i^2 - \left(\sum_{i=1}^{N} X_i \right)^2} \tag{11}$$

$$a_1 = \frac{N \sum_{i=1}^{N} X_i Y_i - \sum_{i=1}^{N} X_i \sum_{i=1}^{N} Y_i}{N \sum_{i=1}^{N} X_i^2 - \left(\sum_{i=1}^{N} X_i \right)^2} \tag{12}$$

The expression for the uncertainty in Y determined by the first-order regression model for a new value of X is found by substituting Eqs. (11) and (12) into

$$Y(X_{new}) = a_0 + a_1 X_{new} \tag{13}$$

and applying the propagation equations. As a result, the general form of the expression for the uncertainty in the predicted value of Y is

$$
\begin{aligned}
U_Y^2 = & \sum_{i=1}^{N}\left(\frac{\partial Y}{\partial Y_i}\right)^2 P_{Y_i}^2 + \sum_{i=1}^{N}\left(\frac{\partial Y}{\partial X_i}\right)^2 P_{X_i}^2 \\
& + \sum_{i=1}^{N}\left(\frac{\partial Y}{\partial Y_i}\right)^2 B_{Y_i}^2 + 2\sum_{i=1}^{N-1}\sum_{k=i+1}^{N}\left(\frac{\partial Y}{\partial Y_i}\right)\left(\frac{\partial Y}{\partial Y_k}\right) B_{Y_i Y_k} \\
& + \sum_{i=1}^{N}\left(\frac{\partial Y}{\partial X_i}\right)^2 B_{X_i}^2 + 2\sum_{i=1}^{N-1}\sum_{k=i+1}^{N}\left(\frac{\partial Y}{\partial X_i}\right)\left(\frac{\partial Y}{\partial X_k}\right) B_{X_i X_k} \\
& + 2\sum_{i=1}^{N}\sum_{k=1}^{N}\left(\frac{\partial Y}{\partial X_i}\right)\left(\frac{\partial Y}{\partial Y_k}\right) B_{X_i Y_k} \\
& + \left(\frac{\partial Y}{\partial X_{new}}\right)^2 P_{new}^2 + \left(\frac{\partial Y}{\partial X_{new}}\right)^2 B_{new}^2 \\
& + 2\sum_{i=1}^{N}\left(\frac{\partial Y}{\partial X_{new}}\right)\left(\frac{\partial Y}{\partial X_i}\right) B_{X_{new} X_i} \\
& + 2\sum_{i=1}^{N}\left(\frac{\partial Y}{\partial X_{new}}\right)\left(\frac{\partial Y}{\partial Y_i}\right) B_{X_{new} Y_i}
\end{aligned}
\tag{14}
$$

The first seven terms account for uncertainties from the original (X_i,Y_i) data pairs. The eighth and ninth terms are from random and systematic uncertainties associated with the new X value. The tenth term accounts for correlated systematic errors between the new X variable and the original X_i variables. The last term accounts for correlated systematic errors between the new X variable and the original Y_i variables.

ANALYSIS OF VARIANCE

The analysis of variance (ANOVA) was used to uncover the main and interaction effects of the independent variables (inlet gas pressure, gravity ratio, and attitude) on the dependent variable (flow rate). A main effect is the direct effect of an independent variable on the dependent variable. An interaction effect is the joint effect of two or more independent variables on the dependent variable. For this experiment, a three-factor ANOVA with replication was performed [8]. The relative importance of a variation source was calculated by using

$$
RI_i = \frac{MS_i}{\sum_{i=1}^{S} MS_i} \tag{15}
$$

where MS_i is the mean square of a variation source.

RESULTS

A typical response of the mass flow meters to gravitational acceleration at 50% of full scale flow in the three orientations is shown in Appendix C. Using Eq. (1), the departure function was calculated for each MFM at all three orientations and gravity levels. Individual plots of the results, shown in Fig. 3, will be discussed in the following sections. The systematic elemental error sources are listed in Table D.1 of Appendix D. The values were either estimated or supplied by the manufacturer. With this information, Eq. (4) was used to calculate the propagated systematic uncertainties. Random uncertainties of the measured variables were found by the method of multiple tests and calculated using Eq. (9). The results are shown in Table D.2 of Appendix D. The total uncertainty of the measured variables and values determined from first-order linear regression models were calculated using Eqs. (10) and (14), respectively. The total uncertainty for each measurement is shown as error bars on the departure functions in Fig. 3. An analysis of variance showing the relative importance for each variation source was calculated from Eq. (15) and will be discussed later. The combined results of all calculations are presented in Appendix E. These results will be presented and discussed in the following text.

The criteria for acceptable performance used in this study was that the departure from orifice flow remain within ±1% of full scale. This was consistent with the manufacturer's specification of accuracy, which includes the effects of non-linearity, hysteresis, and non-repeatability.

In the following sections, the performance of each flow meter will first be discussed individually. Recall that a positive departure function indicates that the MFM reading was less than the orifice flow meter; a negative departure function means the MFM was reading higher than the orifice (see Eq. (1)). Also, because all MFM were calibrated in the orthogonal configuration in normal gravity, the best performance would be expected at this orientation and gravity level. In Fig. 3, note that the scale on the vertical axis has been adjusted for each meter to maintain similar graphical resolution.

After discussing the performance of each meter, the results of the analysis of variance will be presented, followed by a discussion of the overall performance of the mass flow meters.

MKS179A

In normal gravity, the departure function, *i.e.*, the difference between the flow rate measured by the orifice and that measured by the MKS179A, differed by less than ±1% of full scale when the flow meter was in the orthogonal or counterparallel orientations. However, in the coparallel configuration, the departure is greater than 1% of full scale and positive, indicating that the MFM was reading less than the orifice flow meter. If convective heat transfer plays a role in producing these

variations in 1-g, variations with gravity level would also be expected. This was indeed observed, as shown in Fig. 3. However, at both elevated and reduced gravity, the departure function was within ±1% of full scale when the MFM was in the orthogonal (calibrated) orientation. When oriented coparallel, the MKS179A indicated less than the orifice and when counterparallel, it indicated greater than the orifice. In elevated gravity, the departure was greater than ±1% of full scale for all but the lowest flow rate; in reduced gravity, the departure increased with increasing flow rate but was greater than ±1% of full scale only for the highest flow rates.

MKS258C

This meter is also manufactured by MKS so its behavior could be expected to be similar to the MKS179A. However, as shown in Fig. 3, there are significant differences. In the orthogonal orientation, the departure from the orifice reading is within ±1% of full scale for normal and reduced gravity level. For elevated gravity levels, it is within ±1% of full scale for all but the highest flow rates. Co- and counter-parallel orientations at elevated and normal gravity showed large departures from the orifice reading with the MKS258C reading higher than the orifice in the counterparallel orientation and lower than the orifice in the coparallel orientation. The large deviation in flow rate with orientation even in normal gravity emphasizes the importance of using a flow meter in the orientation in which it was calibrated. In spite of this, the departure functions for all orientations are essentially within ±1% of full scale in reduced gravity. This behavior would be expected in the absence of gravity if changes in natural convection was the only cause of the deviations observed in non-zero gravity.

UFM8100

The UFM8100 demonstrated unique behavior in several respects. First, even in the orthogonal (calibrated) orientation at normal gravity, the departure function is greater than ±1% for almost all flow rates. This is indicative of a calibration problem with either the mass flow meter or the reference orifice. Unfortunately, the experimental apparatus was disassembled before this data was analyzed so the cause of this behavior could not be verified. However, this appears to be a systematic effect that could be corrected upon re-calibration. Figure 3 shows the UFM8100 meter demonstrated behavior within about 1.5% of full scale of the orthogonal departure for all orientations. Assuming that conclusions can be drawn based on the effect of attitude and g-level, this indicates that the output of this meter was nearly independent of orientation and gravity level. As with the MKS258C, there was little influence of orientation in reduced gravity.

SI830L

For the SI830L, note that the vertical scale is considerably larger than the other instruments, making the ±1% of full scale band much narrower. In an orthogonal configuration in normal gravity, *i.e.*, the configuration in which it was calibrated, the departure function for the SI830L is within ±1%FS. However, if operated in an off-nominal orientation in normal gravity, the departure function have absolute values of nearly 10% of full scale. In the coparallel orientation, the SI830L reads lower than the orifice while in the counterparallel orientation, it reads higher, similar to the behavior of the MKS179A and MKS258C meters. The behavior of the SI830L at elevated gravity levels is similar to its behavior in normal gravity. In reduced gravity, there is little effect of orientation on the departure function although all three orientations have departure functions greater than ±1% of full scale with the SI830L reading greater than the orifice flow meter. Even though there is little effect of orientation on flow rate in reduced gravity, there appears to be an overall effect of reduced buoyancy on the output of the meter. (This can also be seen in Appendix C in the way the trace of the SI830L output closely mirrors that of the vertical accelerometer.)

HFM200

The behavior of the HFM200 meter is similar to that of the MKS179A meter. The difference is that at normal gravity, the departure functions are within 1%FS for all orientations at all inlet gas pressures. Since there is no effect of orientation on meter output at normal gravity, one might expect the output to also be independent of orientation in reduced gravity. However, as shown in the figure, there is a significant effect with the coparallel configuration having departure functions greater than ±1% of full scale at all inlet pressures. The departure function for the counterparallel configuration is greater than ±1% of full scale only at the highest inlet pressure. The reason for this behavior was not identified although, given the results in normal gravity, it would not appear that it was solely caused by a difference in natural convection.

ANOVA Results

An ANOVA (analysis of variations) was performed on these data to quantify the relative importance of changes in orientation, gravity level, inlet gas pressure, and the interactions between these variables on the values of the departure functions. These results are shown in Table 2. For all meters except the UFM8100, the meter orientation had the largest effect on the departure

function independent of gravity level. This emphasizes the importance of using a mass flow meter in the orientation at which it was calibrated. For these meters, the gravity level was the second highest source of variation but this was generally an order of magnitude less significant than the orientation.

Table 2. Three-Factor ANOVA for Departure Function

Meter	% Relative Importance						
	A	B	C	AB	AC	BC	ABC
MKS179A	86.9	8.92	0.25	2.95	0.84	0.06	0.06
MKS258C	78.2	2.60	1.62	17.1	0.21	0.20	0.09
UFM8100	13.7	23.9	58.7	2.15	1.05	0.23	0.20
SI830L	79.6	1.81	0.12	18.4	0.02	0.02	0.02
HFM200	79.2	2.40	0.16	16.6	1.21	0.06	0.33

A – Orientation
B – Gravity Level
C – Inlet Gas Pressure

The inlet gas pressure had the largest contribution to the departure function for the UFM8100 meter which is indicative of a unit that is out of calibration, as previously discussed. Assuming this is a known source of error that could be eliminated upon re-calibration, the next largest contribution to the error for this meter was the gravity level, not the orientation as for the other meters. This is unique among the meters tested and indicates that the UFM8100 had the least sensitivity to orientation at all gravity levels. For all meters, the effect of joint interactions between inlet gas pressure, orientation, and gravity level were much smaller than the major sources of variation and can be neglected.

DISCUSSION

An ideal flow meter would have an output that was independent of orientation and gravity level. In terms of the departure functions shown in Fig. 3, all the curves for this ideal meter would be coincident and lie within the ±1% FS band. Similar to previous investigations, this study showed flow measurement errors that were dependent on orientation of the meter as well as the magnitude and direction of the gravity vector. Tison [3] had found that the orientation of the meter in normal gravity changed the zero indication by less than 0.44% of full scale and the effect on the span was negligible. The results from the HFM200 and UFM8100 are consistent with this finding. However, the variation in the zero level with orientation in normal gravity ranged from about ±2.5% of full scale for the MKS179A and MKS258C meters and up to ±10% of full scale for the SI830. The MKS179A meter was the only one for which a significant error in the span was observed. The current results are consistent with the those of the previous investigations [3–5] in which variations were observed between meters from different manufacturers. Also, since Tison [3] evaluated meters having considerably lower flow ranges than the meters evaluated in this study, it is plausible that there could be significant variations in the magnitude of the errors.

If differences in buoyancy and therefore, natural convection heat transfer, were the only factor causing the output of thermal flow meters to vary, the effect of orientation would become small in reduced gravity since the g-level is similar in any direction. This type of behavior was observed for the MKS258C, UFM8100, and SI830L instruments but not for the MKS179A or HFM200. Also, if a change in output was caused by buoyancy, the change should become greater in elevated gravity since buoyancy is enhanced in this environment. This behavior was observed for the MKS258C and SI830L; the other meters showed approximately the same behavior in elevated gravity as in normal gravity. Surprisingly, the UFM8100 meter showed similar behavior in all gravity levels with little effect of orientation.

As noted above, the output of the MKS179A and HFM200 instruments was dependent upon orientation even in reduced gravity. This indicates that more complex heat transfer mechanisms exist between the internal components of these instruments. While a detailed evaluation of the design of each flow meter and its heat transfer characteristics was beyond the scope of this study, there are several potential explanations. First, the time scale of the thermal response could be longer than 25 seconds so the meter did not reach a thermal steady-state during the period of reduced gravity. Alternatively, the flow meter could be sensitive to the high-frequency, low amplitude fluctuations in g-level, *i.e.*, g-jitter, that occurs during the low-gravity portions of parabolic flight. The former mechanism was assumed to be negligible because the response time of all instruments was observed to be fast relative to the duration of the low gravity period (see Appendix C). However, the influence of oscillations in g-level was not specifically addressed and could be a factor. This effect could be evaluated in a drop tower where the residual g-level is lower although maintaining instrument calibration and repeatability through the high g-levels experienced at the end of a drop would require special care.

The data obtained in this study also shows that there is no test in normal gravity that will yield conclusive information about how a specific thermal flow meter will respond in either reduced or elevated gravity For four of the five flow meters, the variation in the departure function with inlet gas pressure at elevated

gravity is similar to the variation observed in normal gravity. Therefore, normal gravity behavior is a reasonable indicator of meter performance in elevated gravity. Unfortunately, these results show that the variation of departure function with inlet pressure at reduced gravity may be the same (MKS179A), better (MKS258C, UFM8100, SI830L), or worse (HFM200) than the behavior in normal gravity. In all cases, however, the departure functions at reduced gravity were within about ±5% of full scale. This indicates that all of these meters could be used in reduced gravity if a higher uncertainty is accepted. During operation in long periods of reduced gravity, it is recommended that measures be made to periodically check the calibration of thermal flow meters.

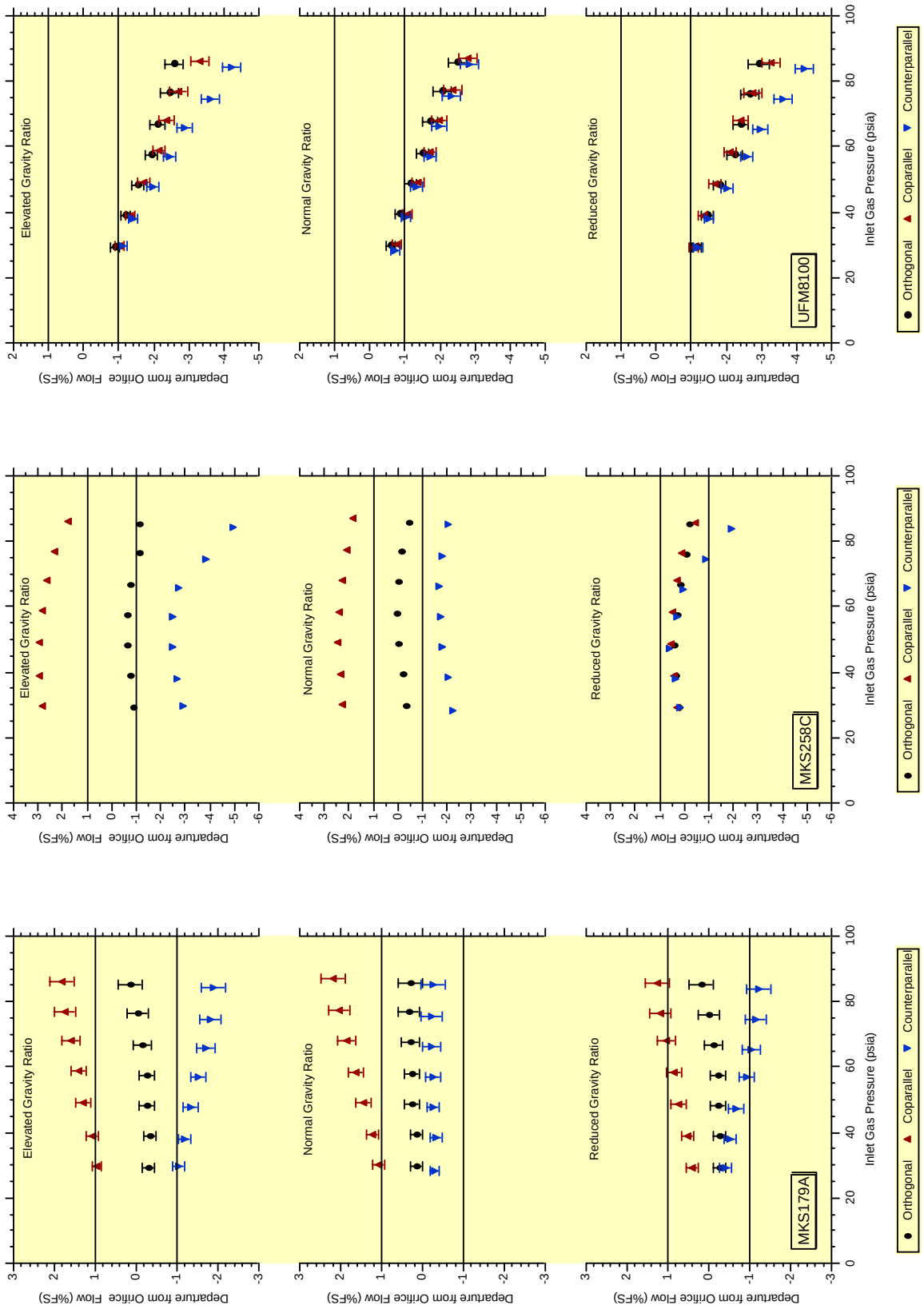

Figure 3. Departure from orifice flow for three flow meter orientations and gravity levels

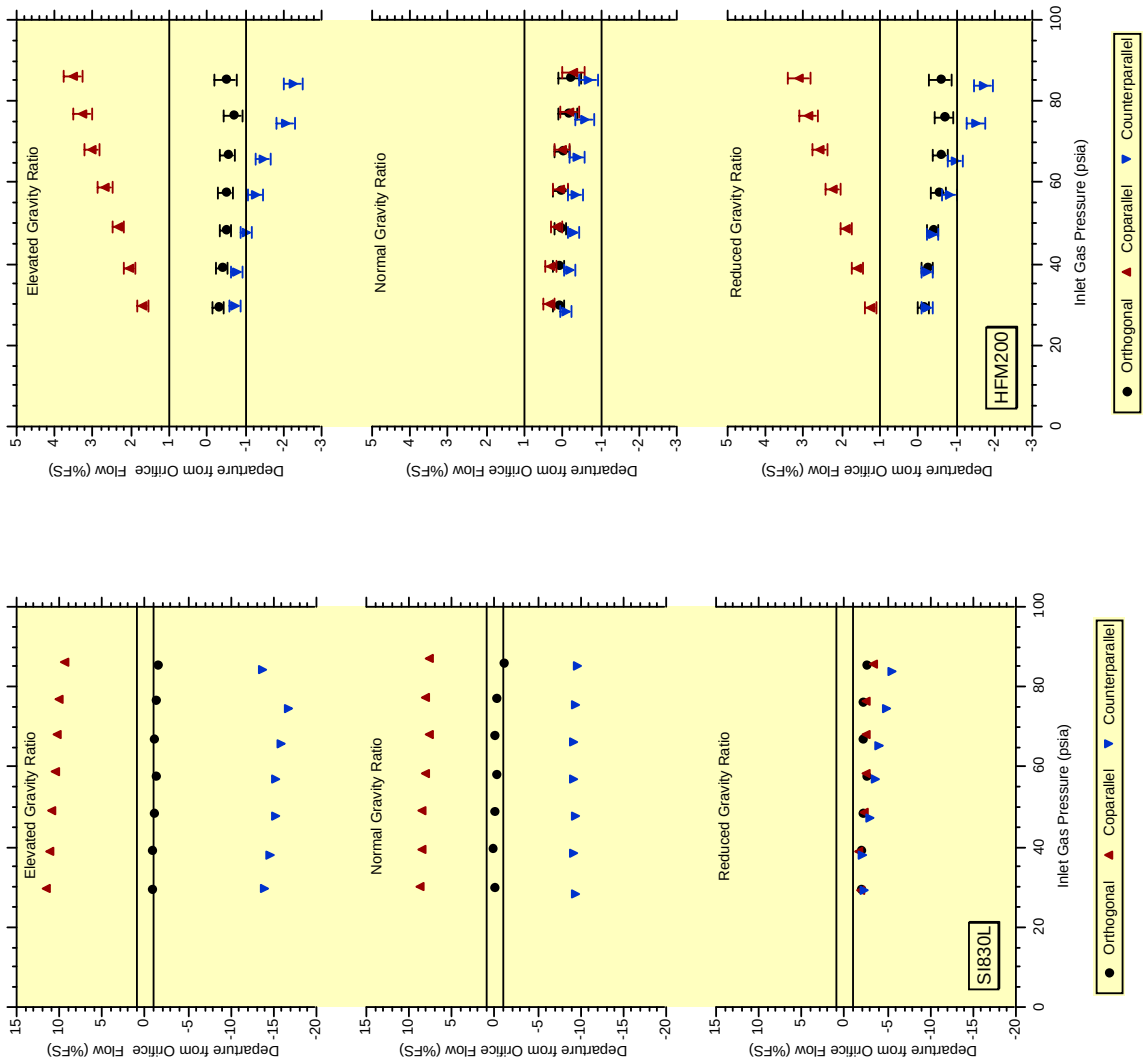

Figure 3. Departure from orifice flow for three flow meter orientations and gravity levels (concluded)

SUMMARY AND CONCLUSIONS

The performance of five thermal mass flow meters were tested on the KC-135 Reduced Gravity Aircraft in orthogonal, coparallel, and counterparallel orientations relative to the **g** vector. Data was taken throughout the parabolic trajectory where the g-level varied from 0.01 to 1.8 times normal gravity. Each meter was calibrated in normal gravity in the orthogonal position prior to flight followed by ground testing at seven different flow conditions to establish a baseline operation. Departure functions relative to an orifice flow reference was developed to quantify the results. A three-factor analysis of variance was performed to uncover the main and interaction effects of the inlet gas pressure, gravity level, and flow meter orientation. A detailed uncertainty analysis was also performed to quantify these effects relative to the systematic and random errors of the experiment.

All of these flow meters performed within manufacturers specifications when operated in normal gravity in the orientation at which they were calibrated. This, of course, is how they were designed and is recommended by the manufacturer. Gravitational acceleration and orientation had a unique effect on the performance of each meter. Specific conclusions from this study are as follows:

1. For only three of the five flow meters did the departure functions for the different orientations converge in reduced gravity. This implies that more complex heat transfer mechanisms exist between the internal components of these instruments than could be evaluated in this experiment. Explanations for this behavior include (1) a transient thermal response such that the meter did not reach steady state during the 25 seconds of reduced gravity on the aircraft or (2) sensitivity to the high-frequency, low amplitude fluctuations in g-level that occurs during the low-gravity portions of parabolic flight.
2. For four of the five meters, the variation in the departure function with orientation at normal gravity was similar to that experienced at elevated gravity. Therefore, meter performance in normal gravity gives a reasonable indication of its performance at elevated gravity levels.
3. The ANOVA analysis indicated that for four of the five meters, variations in the orientation had a greater contribution to the departure function than variations in gravity level. This indicates that if a flow meter will be used in a non-zero gravity environment, the meter should be mounted in the attitude at which it was calibrated.
4. There is no single test that can be performed in normal gravity that will conclusively indicate the reduced gravity performance of a thermal flow meter. Based on this evaluation of five flow meters, the variation of departure function with inlet pressure at reduced gravity may be the same, better, or worse than the behavior in normal gravity.
5. In reduced gravity, the performance of all meters evaluated was within about ±5% of full scale for any orientation, independent of its performance in normal or elevated gravity levels.
6. Even though the flow meters operate on similar principles, their performance was quite different, presumably because of variations in the internal design and details of operation. This emphasizes the need for care in handling thermal flow meters after they have been calibrated. Small changes in configuration, mounting, or internal structure could have dramatic and unexpected effects on their operation and accuracy.

Based on the experience gained during this experiment and the subsequent results, it is suggested that when operating thermal flow meters in low-gravity environments, the greatest accuracy can be obtained by the in-situ calibration of the flow meter.

REFERENCES

[1] Hastings Instruments, *Instruction Manual: 200/202 Series Flow meters/Controllers*, 140–1199, Teledyne Electronic Technologies, Hampton, 1999.

[2] Unit Instruments, *Analog and Digital Mass Flow Controllers and Meters User's Manual*, 199–001–0006 Rev C, Kinetics Electronics, Yorba Linda, 1999.

[3] Tison, S.A. "A Critical Evaluation of Thermal Mass Flow Meters," *J. Vac. Sci. Technol. A*, Vol. 14, No. 4, July/August 1996.

[4] Kondo, Y., Toriyama, N., Matthews, W.A., and Aimedieu, P. "Calibration of the Balloon-Borne NO Instrument," J. Geomag. Geoelectr., Vol. 41, 507–523, 1989.

[5] Weinheimer A.J. and Ridley, B.A. "A Cautionary Note on the Use of Some Mass Flow Controllers," J. Geophysical Research, Vol. 95, No. D7, 9817–9821, 1990.

[6] American National Standards Institute/American Society of Mechanical Engineers, *Test Uncertainty*, PTC 19.1–1998, ASME, New York, 1998.

[7] Coleman, H.W. and Steele, W.G., *Experimentation and Uncertainty Analysis for Engineers*, 2nd ed., John Wiley & Sons, Inc., New York, 1999.

[8] Montgomery, D.C., *Design and Analysis of Experiments*, 4th ed., John Wiley & Sons, Inc., New York, 1997.

APPENDIX A: FLOW SCHEMATIC

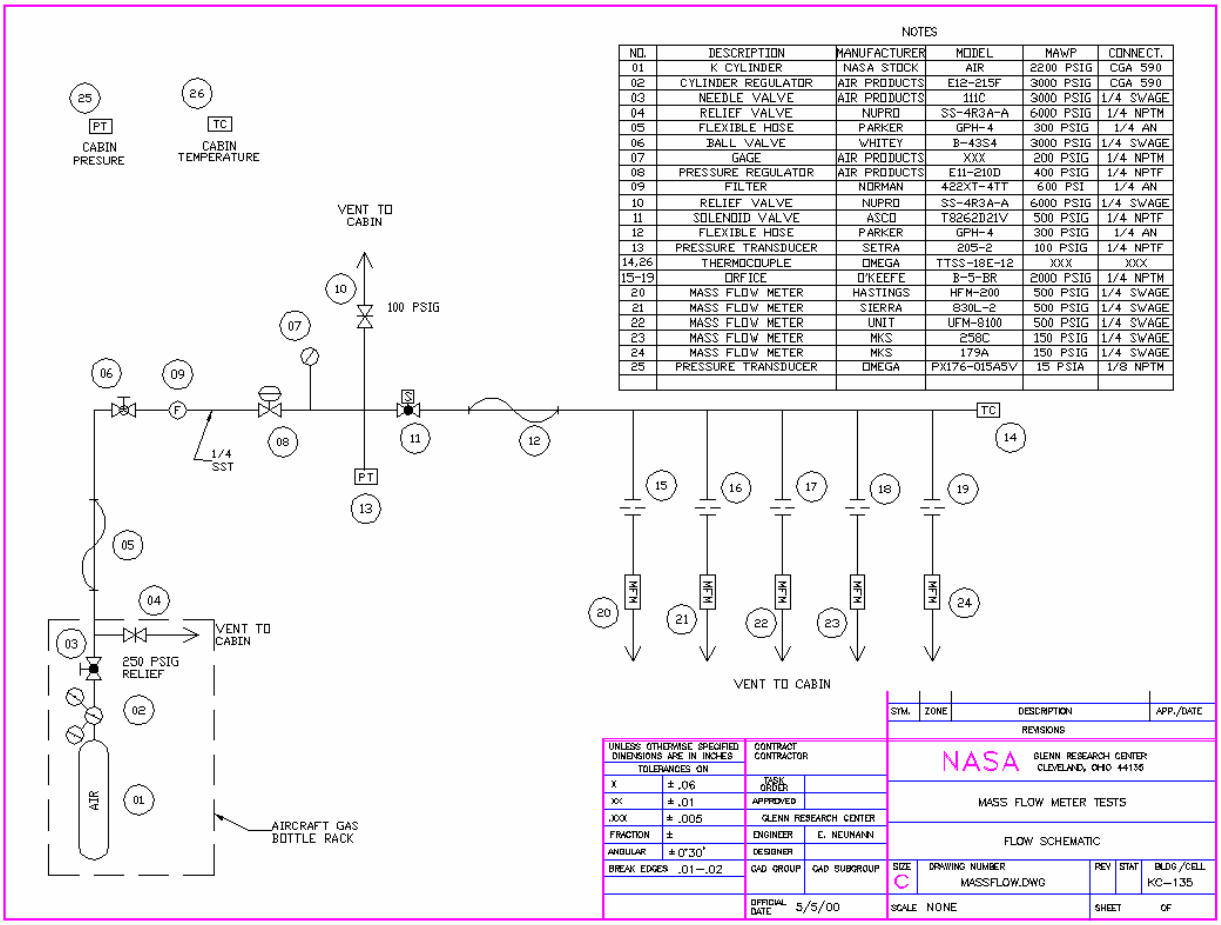

NO.	DESCRIPTION	MANUFACTURER	MODEL	MAWP	CONNECT.
01	K CYLINDER	NASA STOCK	AIR	2200 PSIG	CGA 590
02	CYLINDER REGULATOR	AIR PRODUCTS	E12-215F	3000 PSIG	CGA 590
03	NEEDLE VALVE	AIR PRODUCTS	111C	3000 PSIG	1/4 SWAGE
04	RELIEF VALVE	NUPRO	SS-4R3A-A	6000 PSIG	1/4 NPTM
05	FLEXIBLE HOSE	PARKER	GPH-4	300 PSIG	1/4 AN
06	BALL VALVE	WHITEY	B-43S4	3000 PSIG	1/4 SWAGE
07	GAGE	AIR PRODUCTS	XXX	200 PSIG	1/4 NPTM
08	PRESSURE REGULATOR	AIR PRODUCTS	E11-210D	400 PSIG	1/4 NPTF
09	FILTER	NORMAN	422XT-4TT	600 PSI	1/4 AN
10	RELIEF VALVE	NUPRO	SS-4R3A-A	6000 PSIG	1/4 SWAGE
11	SOLENOID VALVE	ASCO	T8262D21V	500 PSIG	1/4 NPTF
12	FLEXIBLE HOSE	PARKER	GPH-4	300 PSIG	1/4 AN
13	PRESSURE TRANSDUCER	SETRA	205-2	100 PSIG	1/4 NPTF
14,26	THERMOCOUPLE	OMEGA	TTSS-18E-12	XXX	XXX
15-19	ORFICE	O'KEEFE	B-5-BR	2000 PSIG	1/4 NPTM
20	MASS FLOW METER	HASTINGS	HFM-200	500 PSIG	1/4 SWAGE
21	MASS FLOW METER	SIERRA	830L-2	500 PSIG	1/4 SWAGE
22	MASS FLOW METER	UNIT	UFM-8100	500 PSIG	1/4 SWAGE
23	MASS FLOW METER	MKS	258C	150 PSIG	1/4 SWAGE
24	MASS FLOW METER	MKS	179A	150 PSIG	1/4 SWAGE
25	PRESSURE TRANSDUCER	OMEGA	PX176-015A5V	15 PSIA	1/8 NPTM

Figure A.1 Schematic of the flow system used in this experiment

APPENDIX B: CALIBRATION AND MODELS

Table B.1 Calibration Reports with First-Order Linear Regression Models

Device #	Report #	a_0		a_1	
		Value	Units	Value	Units
13	1000046378	-0.005	psia	19.995	psia/VDC
15	421935	-0.01107	slma	0.01047	slma/psia
16	421934	-0.00993	slma	0.01038	slma/psia
17	421933	-0.01081	slma	0.01035	slma/psia
18	421932B	-0.01557	slma	0.01057	slma/psia
19	421931C	-0.01025	slma	0.01080	slma/psia
20	1000048273	5.559E-03	slma	0.1987	slma/VDC
21	1000048272	1.683E-03	slma	0.1998	slma/VDC
22	1000048271	9.158E-04	slma	0.1997	slma/VDC
23	1000048270	-2.132E-03	slma	0.1984	slma/VDC
24	1000048269	6.306E-03	slma	0.1979	slma/VDC
25	1000038626	-2.338	psia	3.018	psia/VDC

Form of Equation: Value = a_1 (Output) + a_0

APPENDIX C: RESPONSE OF THE MASS FLOW METERS

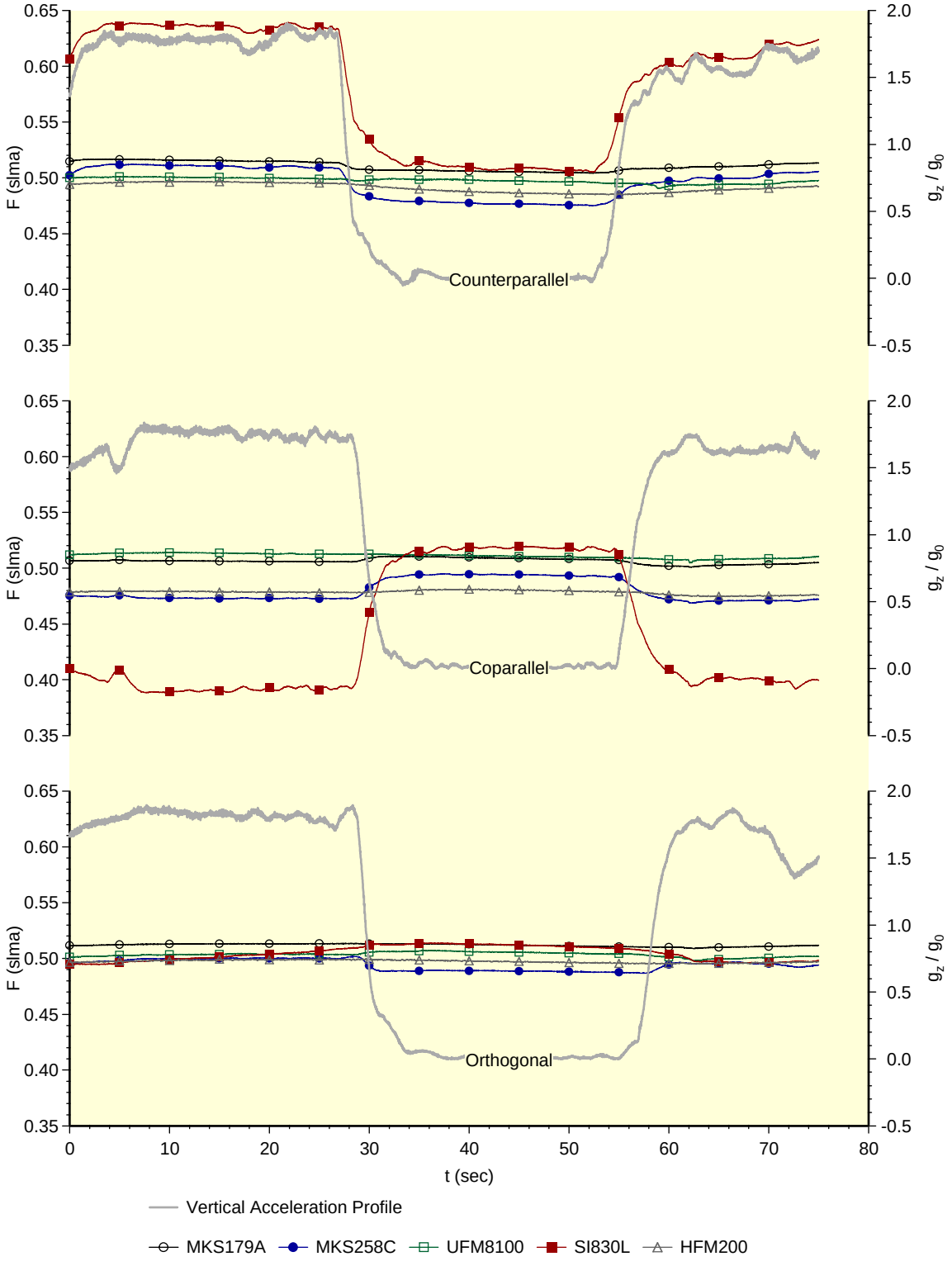

Figure C.1 Response of the MFM gravitational acceleration and attitude (50 %FS)

APPENDIX D: ERROR SOURCES AND UNCERTAINTIES

Table D.1 Systematic Elemental Error Sources

Variable	Source	Notes
F_{mfm}	Calibration	0.2% of reading or 0.02% FS (1 slma), whichever is greater
	DAC	Manufacturer-supplied equation
P_g	Calibration	0.03% FS (100 psia)
	DAC	Manufacturer-supplied equation
P_a	Calibration	0.59% FS (15 psia)
	DAC	Manufacturer-supplied equation
T_g	Calibration	1.0 K (manufacturer)
	DAC	1.0 K (manufacturer)
T_a	Calibration	1.0 K (manufacturer)
	DAC	1.0 K (manufacturer)
g	Calibration	2% FS (2 g_0)
	DAC	Manufacturer-supplied equation

Table D.2 Random Uncertainties

Variable	Ground (normal)	Aircraft (reduced)	Aircraft (elevated)
$F_{MKS179A}$ (slma)	0.000	0.001	0.001
$F_{MKS258C}$ (slma)	0.000	0.001	0.001
$F_{UFM8100}$ (slma)	0.000	0.002	0.001
F_{SI830L} (slma)	0.000	0.003	0.004
F_{HFM200} (slma)	0.000	0.001	0.001
P_g (psia)	0.04	0.08	0.07
P_a (psia)	0.00	0.05	0.04
T_g (°C)	0.0	0.5	0.5
T_a (°C)	0.0	0.7	1.0
g_z/g_0	0.00	0.01	0.02

APPENDIX E: TABULATED RESULTS

The tables in this appendix contains the raw and reduced data for all five mass flow meters, gravity levels, and flow meter attitudes. In all tables, parentheses around numbers indicates a negative value.

Table E.1 Data Table for the Mass Flow Meters in the Orthogonal Orientation

Orthogonal	MKS179A (slma)	MKS258C (slma)	UFM8100 (slma)	SI830L (slma)	HFM200 (slma)	Pg (psia)	Pa (psia)	Tg (°C)	Ta (°C)	g1/g0	g2/g0	g3/g0	Orifice1 (slma)	Orifice2 (slma)	Orifice3 (slma)	Orifice4 (slma)	Orifice5 (slma)	Departure 1 (%FS)	Departure 2 (%FS)	Departure 3 (%FS)	Departure 4 (%FS)	Departure 5 (%FS)
Reduced Gravity																						
Mean	0.307	0.290	0.302	0.312	0.296	29.18	11.99	17.0	17.0	0.02	0.00	0.00	0.305	0.293	0.291	0.293	0.294	(0.2)	0.2	(1.1)	(1.9)	(0.1)
±	0.001	0.001	0.001	0.001	0.001	0.05	0.09	1.4	1.4	0.04	0.04	0.04	0.001	0.001	0.001	0.001	0.001	0.1	0.1	0.1	0.1	0.1
Mean	0.410	0.390	0.404	0.411	0.396	38.68	11.97	17.0	16.6	0.02	0.01	0.01	0.407	0.393	0.389	0.392	0.394	(0.3)	0.3	(1.4)	(1.9)	(0.2)
±	0.001	0.001	0.001	0.001	0.001	0.05	0.10	1.4	1.4	0.04	0.04	0.04	0.001	0.001	0.001	0.001	0.001	0.2	0.1	0.2	0.2	0.2
Mean	0.512	0.489	0.505	0.512	0.497	48.17	11.99	17.2	17.3	0.02	0.00	0.01	0.510	0.493	0.488	0.490	0.493	(0.2)	0.4	(1.8)	(2.2)	(0.4)
±	0.001	0.001	0.001	0.001	0.001	0.05	0.09	1.4	1.4	0.04	0.04	0.04	0.001	0.001	0.001	0.001	0.001	0.2	0.2	0.2	0.2	0.2
Mean	0.613	0.588	0.606	0.612	0.596	57.50	11.93	17.6	17.0	0.02	0.00	0.01	0.610	0.592	0.584	0.587	0.591	(0.2)	0.3	(2.2)	(2.5)	(0.5)
±	0.001	0.001	0.001	0.001	0.001	0.06	0.10	1.4	1.4	0.04	0.04	0.04	0.001	0.001	0.001	0.001	0.001	0.2	0.2	0.2	0.2	0.2
Mean	0.711	0.687	0.704	0.704	0.693	66.74	11.90	18.5	17.8	0.02	0.00	0.00	0.710	0.689	0.680	0.683	0.688	(0.1)	0.2	(2.4)	(2.1)	(0.6)
±	0.002	0.001	0.002	0.002	0.001	0.06	0.10	1.4	1.4	0.04	0.04	0.04	0.002	0.002	0.002	0.002	0.002	0.2	0.2	0.2	0.2	0.2
Mean	0.811	0.789	0.804	0.801	0.792	76.12	11.95	19.3	18.3	0.02	0.00	0.00	0.811	0.788	0.777	0.780	0.786	0.0	(0.1)	(2.7)	(2.1)	(0.7)
±	0.002	0.002	0.002	0.002	0.002	0.06	0.10	1.4	1.4	0.04	0.04	0.04	0.002	0.002	0.002	0.002	0.002	0.3	0.2	0.3	0.3	0.2
Mean	0.906	0.884	0.898	0.897	0.885	85.05	11.94	20.5	20.1	0.02	0.01	0.00	0.908	0.882	0.869	0.873	0.879	0.2	(0.2)	(2.9)	(2.4)	(0.6)
±	0.002	0.002	0.002	0.002	0.002	0.07	0.10	1.4	1.4	0.04	0.04	0.04	0.002	0.002	0.002	0.002	0.002	0.3	0.3	0.3	0.3	0.3
Normal Gravity																						
Mean	0.308	0.300	0.301	0.296	0.297	29.59	14.39	22.3	24.8	0.03	0.07	1.01	0.309	0.297	0.295	0.297	0.299	0.1	(0.3)	(0.6)	0.2	0.1
±	0.001	0.001	0.001	0.001	0.001	0.04	0.09	1.4	1.4	0.04	0.04	0.04	0.001	0.001	0.001	0.001	0.001	0.1	0.1	0.1	0.1	0.1
Mean	0.412	0.401	0.404	0.394	0.399	39.26	14.39	22.3	24.8	0.03	0.07	1.01	0.414	0.399	0.395	0.398	0.400	0.2	(0.2)	(0.8)	0.4	0.1
±	0.001	0.001	0.001	0.001	0.001	0.04	0.09	1.4	1.4	0.04	0.04	0.04	0.001	0.001	0.001	0.001	0.001	0.1	0.1	0.1	0.1	0.1
Mean	0.513	0.498	0.504	0.494	0.498	48.68	14.39	22.2	24.7	0.03	0.07	1.01	0.515	0.498	0.493	0.496	0.498	0.2	(0.0)	(1.1)	0.2	0.1
±	0.001	0.001	0.001	0.001	0.001	0.04	0.09	1.4	1.4	0.04	0.04	0.04	0.001	0.001	0.001	0.001	0.001	0.2	0.2	0.2	0.2	0.2
Mean	0.614	0.597	0.605	0.594	0.596	58.05	14.39	22.2	24.7	0.03	0.07	1.01	0.616	0.597	0.590	0.593	0.597	0.3	0.0	(1.5)	(0.2)	0.1
±	0.001	0.001	0.001	0.001	0.001	0.05	0.09	1.4	1.4	0.04	0.04	0.04	0.001	0.001	0.001	0.001	0.001	0.2	0.2	0.2	0.2	0.2
Mean	0.715	0.697	0.705	0.690	0.695	67.49	14.39	22.1	24.6	0.03	0.07	1.01	0.718	0.697	0.687	0.691	0.695	0.3	0.0	(1.7)	0.1	0.0
±	0.002	0.001	0.001	0.001	0.001	0.05	0.09	1.4	1.4	0.04	0.04	0.04	0.002	0.002	0.002	0.002	0.002	0.2	0.2	0.2	0.2	0.2
Mean	0.814	0.796	0.804	0.788	0.793	76.71	14.39	22.1	24.5	0.03	0.07	1.01	0.818	0.794	0.783	0.787	0.792	0.3	(0.1)	(2.1)	(0.1)	(0.1)
±	0.002	0.002	0.002	0.002	0.002	0.05	0.09	1.4	1.4	0.04	0.04	0.04	0.002	0.002	0.002	0.002	0.002	0.3	0.2	0.2	0.2	0.2
Mean	0.912	0.894	0.901	0.889	0.888	85.70	14.39	22.0	24.5	0.03	0.07	1.01	0.915	0.889	0.876	0.880	0.886	0.3	(0.4)	(2.5)	(0.9)	(0.2)
±	0.002	0.002	0.002	0.002	0.002	0.05	0.09	1.4	1.4	0.04	0.04	0.04	0.002	0.002	0.002	0.002	0.002	0.3	0.3	0.3	0.3	0.3
Elevated Gravity																						
Mean	0.309	0.303	0.302	0.302	0.299	29.33	12.22	17.0	17.1	0.01	0.20	1.83	0.306	0.294	0.293	0.295	0.296	(0.3)	(0.9)	(0.9)	(0.7)	(0.3)
±	0.001	0.001	0.001	0.002	0.001	0.04	0.09	1.4	1.4	0.04	0.04	0.04	0.001	0.001	0.001	0.001	0.001	0.1	0.1	0.1	0.2	0.1
Mean	0.412	0.402	0.402	0.402	0.399	38.78	12.18	17.1	17.0	0.02	0.22	1.83	0.408	0.394	0.390	0.393	0.395	(0.3)	(0.8)	(1.2)	(0.9)	(0.4)
±	0.001	0.001	0.001	0.001	0.001	0.04	0.09	1.4	1.4	0.04	0.04	0.04	0.001	0.001	0.001	0.001	0.001	0.1	0.1	0.1	0.2	0.1
Mean	0.513	0.500	0.504	0.501	0.499	48.23	12.19	17.3	17.3	0.01	0.20	1.83	0.510	0.494	0.488	0.491	0.494	(0.3)	(0.6)	(1.6)	(1.1)	(0.5)
±	0.001	0.001	0.001	0.002	0.001	0.04	0.09	1.4	1.4	0.04	0.04	0.04	0.001	0.001	0.001	0.001	0.001	0.2	0.2	0.2	0.2	0.2
Mean	0.614	0.598	0.604	0.601	0.596	57.54	12.09	17.7	17.5	0.02	0.19	1.83	0.611	0.592	0.584	0.588	0.591	(0.3)	(0.6)	(1.9)	(1.3)	(0.5)
±	0.001	0.001	0.001	0.002	0.001	0.05	0.09	1.4	1.4	0.04	0.04	0.04	0.001	0.001	0.001	0.001	0.001	0.2	0.2	0.2	0.2	0.2
Mean	0.713	0.698	0.702	0.693	0.694	66.82	12.12	18.5	18.3	0.01	0.19	1.85	0.711	0.690	0.680	0.684	0.688	(0.2)	(0.8)	(2.1)	(0.9)	(0.5)
±	0.002	0.002	0.002	0.002	0.001	0.05	0.09	1.4	1.4	0.04	0.04	0.04	0.002	0.002	0.002	0.002	0.002	0.2	0.2	0.2	0.2	0.2
Mean	0.814	0.802	0.803	0.795	0.795	76.34	12.30	19.4	18.4	0.01	0.20	1.82	0.814	0.791	0.779	0.783	0.788	(0.1)	(1.1)	(2.4)	(1.2)	(0.7)
±	0.002	0.002	0.002	0.002	0.002	0.05	0.09	1.4	1.4	0.04	0.04	0.04	0.002	0.002	0.002	0.002	0.002	0.3	0.2	0.2	0.3	0.2
Mean	0.907	0.895	0.896	0.888	0.885	85.15	12.05	20.6	20.5	0.02	0.17	1.85	0.909	0.884	0.870	0.874	0.880	0.2	(1.1)	(2.6)	(1.4)	(0.5)
±	0.002	0.002	0.002	0.002	0.002	0.06	0.10	1.4	1.4	0.04	0.04	0.04	0.002	0.002	0.002	0.002	0.002	0.3	0.3	0.3	0.3	0.3

Table E.2 Data Table for the Mass Flow Meters in the Coparallel Orientation

Coparallel	MKS179A (slma)	MKS258C (slma)	UFM8100 (slma)	SI830L (slma)	HFM200 (slma)	Pg (psia)	Pa (psia)	Tg (°C)	Ta (°C)	g1/g0	g2/g0	g3/g0	Orifice1 (slma)	Orifice2 (slma)	Orifice3 (slma)	Orifice4 (slma)	Orifice5 (slma)	Departure 1 (%FS)	Departure 2 (%FS)	Departure 3 (%FS)	Departure 4 (%FS)	Departure 5 (%FS)
Reduced Gravity																						
Mean	0.303	0.292	0.304	0.314	0.284	29.38	12.01	19.0	19.4	0.02	(0.00)	(0.00)	0.307	0.295	0.293	0.295	0.297	0.4	0.3	(1.1)	(1.9)	1.2
±	0.001	0.001	0.001	0.001	0.001	0.05	0.09	1.4	1.4	0.04	0.04	0.04	0.001	0.001	0.001	0.001	0.001	0.1	0.1	0.1	0.1	0.1
Mean	0.403	0.389	0.403	0.409	0.379	38.75	12.05	19.0	19.3	0.02	0.01	(0.01)	0.408	0.394	0.390	0.392	0.395	0.5	0.5	(1.3)	(1.6)	1.6
±	0.001	0.001	0.001	0.002	0.001	0.05	0.09	1.4	1.4	0.04	0.04	0.04	0.001	0.001	0.001	0.001	0.001	0.2	0.1	0.1	0.2	0.1
Mean	0.509	0.494	0.511	0.519	0.480	48.77	11.97	18.8	19.3	0.02	(0.02)	(0.00)	0.516	0.499	0.494	0.496	0.499	0.7	0.5	(1.7)	(2.2)	1.9
±	0.001	0.001	0.001	0.001	0.001	0.05	0.09	1.4	1.4	0.04	0.04	0.04	0.001	0.001	0.001	0.001	0.001	0.2	0.2	0.2	0.2	0.2
Mean	0.611	0.596	0.614	0.620	0.577	58.37	11.92	18.7	19.2	0.03	0.00	0.00	0.620	0.601	0.593	0.596	0.600	0.9	0.5	(2.1)	(2.4)	2.3
±	0.001	0.001	0.001	0.002	0.001	0.05	0.09	1.4	1.4	0.04	0.04	0.04	0.001	0.001	0.001	0.001	0.001	0.2	0.2	0.2	0.2	0.2
Mean	0.713	0.699	0.716	0.719	0.674	67.92	11.97	18.7	19.4	0.01	(0.01)	(0.00)	0.723	0.702	0.692	0.695	0.700	1.0	0.3	(2.4)	(2.4)	2.6
±	0.002	0.001	0.002	0.002	0.001	0.06	0.09	1.4	1.4	0.04	0.04	0.04	0.002	0.002	0.002	0.002	0.002	0.2	0.2	0.2	0.2	0.2
Mean	0.803	0.791	0.808	0.809	0.760	76.45	11.98	18.6	19.4	0.02	0.00	(0.00)	0.815	0.792	0.780	0.784	0.789	1.2	0.1	(2.7)	(2.5)	2.9
±	0.002	0.002	0.002	0.002	0.002	0.06	0.09	1.4	1.4	0.04	0.04	0.04	0.002	0.002	0.002	0.002	0.002	0.3	0.2	0.2	0.3	0.2
Mean	0.903	0.895	0.909	0.914	0.855	85.75	11.94	18.3	19.5	0.02	(0.01)	(0.00)	0.915	0.890	0.876	0.880	0.887	1.3	(0.5)	(3.3)	(3.4)	3.1
±	0.002	0.002	0.002	0.002	0.002	0.06	0.09	1.4	1.4	0.04	0.04	0.04	0.002	0.002	0.002	0.002	0.002	0.3	0.3	0.3	0.3	0.3
Normal Gravity																						
Mean	0.303	0.279	0.307	0.214	0.299	29.99	14.29	21.9	23.1	0.07	1.01	0.01	0.313	0.301	0.299	0.301	0.303	1.1	2.2	(0.8)	8.7	0.3
±	0.001	0.001	0.001	0.001	0.001	0.04	0.09	1.4	1.4	0.04	0.04	0.04	0.001	0.001	0.001	0.001	0.001	0.1	0.1	0.1	0.1	0.1
Mean	0.405	0.379	0.409	0.316	0.400	39.57	14.29	21.8	22.9	0.07	1.01	0.01	0.417	0.402	0.399	0.401	0.403	1.2	2.3	(1.1)	8.5	0.3
±	0.001	0.001	0.001	0.001	0.001	0.04	0.09	1.4	1.4	0.04	0.04	0.04	0.001	0.001	0.001	0.001	0.001	0.1	0.1	0.1	0.1	0.1
Mean	0.504	0.478	0.510	0.414	0.501	49.03	14.30	21.8	22.9	0.07	1.01	0.01	0.519	0.502	0.496	0.499	0.502	1.5	2.4	(1.4)	8.6	0.2
±	0.001	0.001	0.001	0.001	0.001	0.04	0.09	1.4	1.4	0.04	0.04	0.04	0.001	0.001	0.001	0.001	0.001	0.2	0.2	0.2	0.2	0.2
Mean	0.605	0.579	0.612	0.516	0.601	58.54	14.30	21.8	22.8	0.07	1.01	0.01	0.622	0.603	0.595	0.598	0.602	1.6	2.4	(1.7)	8.2	0.1
±	0.001	0.001	0.001	0.001	0.001	0.05	0.09	1.4	1.4	0.04	0.04	0.04	0.001	0.001	0.001	0.001	0.001	0.2	0.2	0.2	0.2	0.2
Mean	0.708	0.682	0.715	0.621	0.703	68.21	14.30	21.8	22.8	0.07	1.01	0.01	0.726	0.705	0.695	0.698	0.703	1.8	2.3	(2.0)	7.7	(0.0)
±	0.001	0.001	0.001	0.001	0.001	0.05	0.09	1.4	1.4	0.04	0.04	0.04	0.002	0.002	0.002	0.002	0.002	0.2	0.2	0.2	0.2	0.2
Mean	0.806	0.782	0.815	0.715	0.802	77.50	14.30	21.8	22.8	0.07	1.01	0.01	0.826	0.803	0.791	0.795	0.800	2.0	2.1	(2.4)	8.0	(0.2)
±	0.002	0.002	0.002	0.001	0.002	0.05	0.09	1.4	1.4	0.04	0.04	0.04	0.002	0.002	0.002	0.002	0.002	0.3	0.2	0.2	0.2	0.2
Mean	0.909	0.887	0.919	0.820	0.905	87.21	14.30	21.9	22.7	0.07	1.01	0.01	0.931	0.905	0.891	0.896	0.902	2.2	1.8	(2.8)	7.5	(0.3)
±	0.002	0.002	0.002	0.002	0.002	0.05	0.09	1.4	1.4	0.04	0.04	0.04	0.002	0.002	0.002	0.002	0.002	0.3	0.3	0.3	0.3	0.3
Elevated Gravity																						
Mean	0.300	0.269	0.306	0.183	0.282	29.61	12.27	18.9	19.4	0.11	1.80	(0.04)	0.309	0.297	0.295	0.298	0.299	1.0	2.8	(1.0)	11.5	1.7
±	0.001	0.001	0.001	0.001	0.001	0.04	0.09	1.4	1.4	0.04	0.04	0.04	0.001	0.001	0.001	0.001	0.001	0.1	0.1	0.1	0.1	0.1
Mean	0.399	0.366	0.405	0.283	0.376	38.95	12.27	19.0	19.4	0.10	1.80	(0.04)	0.410	0.396	0.392	0.395	0.397	1.1	2.9	(1.3)	11.2	2.1
±	0.001	0.001	0.001	0.001	0.001	0.04	0.09	1.4	1.4	0.04	0.04	0.04	0.001	0.001	0.001	0.001	0.001	0.1	0.1	0.1	0.2	0.1
Mean	0.506	0.473	0.514	0.391	0.479	49.04	12.26	18.8	19.5	0.10	1.77	(0.05)	0.519	0.502	0.497	0.499	0.502	1.3	2.9	(1.7)	10.9	2.4
±	0.001	0.001	0.001	0.001	0.001	0.05	0.09	1.4	1.4	0.04	0.04	0.04	0.001	0.001	0.001	0.001	0.001	0.2	0.2	0.2	0.2	0.2
Mean	0.609	0.576	0.618	0.495	0.576	58.67	12.23	18.7	19.3	0.10	1.77	(0.05)	0.623	0.604	0.596	0.599	0.603	1.4	2.8	(2.1)	10.4	2.7
±	0.001	0.001	0.001	0.002	0.001	0.05	0.09	1.4	1.4	0.04	0.04	0.04	0.001	0.001	0.001	0.001	0.001	0.2	0.2	0.2	0.2	0.2
Mean	0.710	0.679	0.719	0.596	0.673	68.23	12.26	18.7	19.5	0.11	1.80	(0.04)	0.726	0.705	0.695	0.699	0.703	1.6	2.6	(2.4)	10.3	3.0
±	0.001	0.001	0.002	0.002	0.001	0.05	0.09	1.4	1.4	0.04	0.04	0.04	0.002	0.002	0.002	0.002	0.002	0.2	0.2	0.2	0.3	0.2
Mean	0.800	0.771	0.810	0.687	0.759	76.72	12.25	18.6	19.5	0.11	1.76	(0.02)	0.818	0.795	0.783	0.787	0.792	1.7	2.3	(2.7)	10.0	3.3
±	0.002	0.002	0.002	0.002	0.002	0.05	0.09	1.4	1.4	0.04	0.04	0.04	0.002	0.002	0.002	0.002	0.002	0.2	0.2	0.2	0.2	0.2
Mean	0.900	0.875	0.913	0.790	0.854	86.05	12.22	18.2	19.5	0.10	1.80	(0.05)	0.919	0.893	0.879	0.884	0.890	1.8	1.8	(3.3)	9.4	3.5
±	0.002	0.002	0.002	0.002	0.002	0.05	0.09	1.4	1.4	0.04	0.04	0.04	0.002	0.002	0.002	0.002	0.002	0.3	0.3	0.3	0.3	0.3

Table E.3 Data Table for the Mass Flow Meters in the Counterparallel Orientation

Counterparallel	MKS179A (slma)	MKS258C (slma)	UFM8100 (slma)	SI830L (slma)	HFM200 (slma)	Pg (psia)	Pa (psia)	Tg (°C)	Ta (°C)	g1/g0	g2/g0	g3/g0	Orifice1 (slma)	Orifice2 (slma)	Orifice3 (slma)	Orifice4 (slma)	Orifice5 (slma)	Departure 1 (%FS)	Departure 2 (%FS)	Departure 3 (%FS)	Departure 4 (%FS)	Departure 5 (%FS)
Reduced Gravity																						
Mean	0.309	0.292	0.304	0.316	0.297	29.25	12.09	15.5	17.2	0.02	0.00	(0.01)	0.305	0.293	0.292	0.294	0.295	(0.4)	0.2	(1.2)	(2.2)	(0.2)
±	0.001	0.001	0.001	0.002	0.001	0.05	0.10	1.4	1.4	0.04	0.04	0.04	0.001	0.001	0.001	0.001	0.001	0.1	0.1	0.1	0.2	0.2
Mean	0.404	0.380	0.396	0.405	0.388	37.85	12.03	15.4	17.2	0.02	0.00	(0.01)	0.398	0.384	0.381	0.383	0.385	(0.5)	0.4	(1.5)	(2.2)	(0.2)
±	0.001	0.001	0.001	0.002	0.001	0.05	0.09	1.4	1.4	0.04	0.04	0.04	0.001	0.001	0.001	0.001	0.001	0.2	0.1	0.1	0.2	0.2
Mean	0.505	0.476	0.497	0.508	0.486	47.15	11.96	13.6	17.2	0.03	0.00	(0.00)	0.499	0.482	0.477	0.480	0.483	(0.7)	0.6	(2.0)	(2.8)	(0.4)
±	0.001	0.001	0.001	0.001	0.001	0.05	0.09	1.4	1.4	0.04	0.04	0.04	0.001	0.001	0.001	0.001	0.001	0.2	0.2	0.2	0.2	0.2
Mean	0.611	0.581	0.602	0.615	0.591	56.73	12.02	12.4	14.6	0.03	(0.00)	(0.00)	0.602	0.583	0.576	0.579	0.583	(0.9)	0.3	(2.6)	(3.6)	(0.8)
±	0.001	0.001	0.001	0.002	0.001	0.05	0.09	1.4	1.4	0.04	0.04	0.04	0.001	0.001	0.001	0.001	0.001	0.2	0.2	0.2	0.2	0.2
Mean	0.707	0.675	0.696	0.710	0.684	65.48	12.02	12.0	15.0	0.03	0.01	(0.01)	0.697	0.676	0.667	0.670	0.674	(1.0)	0.0	(3.0)	(4.0)	(1.0)
±	0.002	0.002	0.002	0.002	0.002	0.06	0.09	1.4	1.4	0.04	0.04	0.04	0.002	0.002	0.002	0.002	0.002	0.2	0.2	0.2	0.3	0.2
Mean	0.806	0.781	0.797	0.813	0.785	74.58	12.01	10.6	13.7	0.03	0.01	(0.01)	0.795	0.772	0.761	0.764	0.770	(1.1)	(0.9)	(3.6)	(4.8)	(1.5)
±	0.002	0.002	0.002	0.003	0.002	0.05	0.09	1.4	1.4	0.04	0.04	0.04	0.002	0.002	0.002	0.002	0.002	0.2	0.2	0.2	0.3	0.2
Mean	0.908	0.890	0.900	0.917	0.885	83.91	12.01	10.6	13.0	0.03	(0.01)	(0.01)	0.896	0.871	0.857	0.861	0.867	(1.2)	(1.9)	(4.2)	(5.6)	(1.7)
±	0.002	0.002	0.002	0.002	0.002	0.06	0.09	1.4	1.4	0.04	0.04	0.04	0.002	0.002	0.002	0.002	0.002	0.3	0.3	0.3	0.3	0.3
Normal Gravity																						
Mean	0.298	0.305	0.289	0.377	0.286	28.26	14.29	21.3	23.0	(0.02)	0.99	(0.01)	0.295	0.283	0.282	0.284	0.285	(0.3)	(2.2)	(0.7)	(9.3)	(0.1)
±	0.001	0.001	0.001	0.001	0.001	0.04	0.09	1.4	1.4	0.04	0.04	0.04	0.001	0.001	0.001	0.001	0.001	0.1	0.1	0.1	0.1	0.1
Mean	0.406	0.409	0.395	0.480	0.391	38.21	14.29	21.2	22.9	(0.02)	0.99	(0.01)	0.402	0.388	0.385	0.387	0.389	(0.3)	(2.1)	(1.0)	(9.3)	(0.2)
±	0.001	0.001	0.001	0.001	0.001	0.04	0.09	1.4	1.4	0.04	0.04	0.04	0.001	0.001	0.001	0.001	0.001	0.1	0.1	0.1	0.2	0.1
Mean	0.506	0.505	0.495	0.579	0.490	47.58	14.29	21.1	22.9	(0.02)	0.99	(0.01)	0.503	0.487	0.481	0.484	0.487	(0.3)	(1.8)	(1.3)	(9.5)	(0.3)
±	0.001	0.001	0.001	0.001	0.001	0.04	0.09	1.4	1.4	0.04	0.04	0.04	0.001	0.001	0.001	0.001	0.001	0.2	0.2	0.2	0.2	0.2
Mean	0.609	0.605	0.597	0.676	0.590	57.12	14.29	21.0	22.8	(0.02)	0.99	(0.01)	0.606	0.588	0.580	0.583	0.587	(0.2)	(1.7)	(1.7)	(9.2)	(0.3)
±	0.001	0.001	0.001	0.001	0.001	0.04	0.09	1.4	1.4	0.04	0.04	0.04	0.001	0.001	0.001	0.001	0.001	0.2	0.2	0.2	0.2	0.2
Mean	0.709	0.703	0.696	0.772	0.688	66.41	14.29	20.9	22.8	(0.02)	0.99	(0.01)	0.707	0.686	0.676	0.680	0.684	(0.2)	(1.7)	(2.0)	(9.2)	(0.4)
±	0.001	0.001	0.001	0.002	0.001	0.05	0.09	1.4	1.4	0.04	0.04	0.04	0.002	0.002	0.002	0.002	0.002	0.2	0.2	0.2	0.2	0.2
Mean	0.805	0.798	0.792	0.868	0.784	75.37	14.29	20.8	22.8	(0.02)	0.99	(0.01)	0.803	0.780	0.769	0.773	0.778	(0.2)	(1.8)	(2.3)	(9.5)	(0.6)
±	0.002	0.002	0.002	0.002	0.002	0.05	0.09	1.4	1.4	0.04	0.04	0.04	0.002	0.002	0.002	0.002	0.002	0.2	0.2	0.2	0.3	0.2
Mean	0.910	0.903	0.897	0.969	0.886	85.04	14.29	20.6	22.7	(0.02)	0.99	(0.01)	0.908	0.882	0.869	0.873	0.879	(0.3)	(2.1)	(2.8)	(9.6)	(0.7)
±	0.002	0.002	0.002	0.002	0.002	0.05	0.09	1.4	1.4	0.04	0.04	0.04	0.002	0.002	0.002	0.002	0.002	0.3	0.3	0.3	0.3	0.3
Elevated Gravity																						
Mean	0.317	0.324	0.305	0.436	0.304	29.41	12.27	15.5	17.2	(0.03)	1.75	(0.08)	0.307	0.295	0.293	0.295	0.297	(1.0)	(2.9)	(1.1)	(14.0)	(0.7)
±	0.001	0.001	0.001	0.001	0.001	0.04	0.09	1.4	1.4	0.04	0.04	0.04	0.001	0.001	0.001	0.001	0.001	0.1	0.1	0.1	0.2	0.1
Mean	0.413	0.414	0.398	0.531	0.396	38.10	12.30	15.4	17.3	(0.03)	1.79	(0.08)	0.401	0.387	0.383	0.386	0.388	(1.2)	(2.7)	(1.4)	(14.6)	(0.8)
±	0.001	0.001	0.001	0.001	0.001	0.04	0.09	1.4	1.4	0.04	0.04	0.04	0.001	0.001	0.001	0.001	0.001	0.1	0.1	0.1	0.2	0.1
Mean	0.516	0.511	0.501	0.637	0.496	47.51	12.36	13.3	17.3	(0.03)	1.78	(0.08)	0.503	0.486	0.481	0.483	0.486	(1.3)	(2.5)	(2.0)	(15.3)	(1.0)
±	0.001	0.001	0.001	0.002	0.001	0.05	0.09	1.4	1.4	0.04	0.04	0.04	0.001	0.001	0.001	0.001	0.001	0.2	0.2	0.2	0.2	0.2
Mean	0.619	0.611	0.603	0.733	0.598	56.92	12.23	12.4	15.0	(0.04)	1.77	(0.09)	0.604	0.586	0.578	0.581	0.585	(1.5)	(2.5)	(2.5)	(15.2)	(1.3)
±	0.001	0.001	0.001	0.002	0.001	0.05	0.09	1.4	1.4	0.04	0.04	0.04	0.001	0.001	0.001	0.001	0.001	0.2	0.2	0.2	0.2	0.2
Mean	0.715	0.705	0.697	0.829	0.690	65.62	12.23	11.9	15.0	(0.03)	1.78	(0.07)	0.698	0.677	0.668	0.671	0.676	(1.7)	(2.8)	(2.9)	(15.8)	(1.5)
±	0.002	0.002	0.001	0.002	0.001	0.05	0.09	1.4	1.4	0.04	0.04	0.04	0.002	0.002	0.002	0.002	0.002	0.2	0.2	0.2	0.3	0.2
Mean	0.814	0.811	0.798	0.934	0.792	74.71	12.25	10.5	13.7	(0.03)	1.79	(0.10)	0.796	0.773	0.762	0.766	0.771	(1.8)	(3.8)	(3.6)	(16.8)	(2.1)
±	0.002	0.002	0.002	0.002	0.002	0.05	0.09	1.4	1.4	0.04	0.04	0.04	0.002	0.002	0.002	0.002	0.002	0.2	0.2	0.2	0.3	0.2
Mean	0.917	0.922	0.902	1.001	0.893	84.17	12.34	10.7	13.1	(0.03)	1.76	(0.11)	0.898	0.873	0.860	0.864	0.870	(1.9)	(4.9)	(4.2)	(13.7)	(2.3)
±	0.002	0.002	0.002	0.002	0.002	0.06	0.09	1.4	1.4	0.04	0.04	0.04	0.002	0.002	0.002	0.002	0.002	0.3	0.3	0.3	0.3	0.3

APPENDIX F: SYMBOLS

a_n	coefficients of linear regression model
B_i	estimate of systematic uncertainty at a 95% confidence limit for i^{th} measured variable
B_J	systematic uncertainty for measured variable J
B_r	systematic uncertainty of result
B_{ik}	covariance estimator for L correlated (common) elemental systematic error sources for measurements of variables X_i and X_k
DAC	data acquisition and control
D	departure function
F	mass flow rate
FS	full scale
$\boldsymbol{g}$	gravitational acceleration vector
g_0	vertical gravitational acceleration at surface
g_z	vertical gravitational acceleration
Hz	hertz
J	total number of measured variables
L	total number of elemental systematic error sources common for measurements of variables X_i and X_k
M	total number of elemental error sources; total number of replications
MFM, mfm	mass flow meter
MS_i	mean square of a variation source
N	number of data pairs
orf	orifice
P_a	ambient pressure
P_g	gas pressure
$P_{\bar{r}}$	random uncertainty of mean result
r	experimental result determined from J measured variables
$\bar{r}$	mean value of result from replicating a single test M times
RI_i	relative importance of a variation source
S_r	standard deviation of sample population of M individual tests
$S_{\bar{r}}$	standard deviation of mean result from M tests
sccm	standard cubic meters per minute air
slma	standard liters per minute air
t	t-distribution
T_a	ambient temperature
T_g	gas temperature

VDC	volt direct current
$U_{\bar{r}}$	total uncertainty of mean result
U_Y	total uncertainty of y-value determine from the first-order linear regression model
X_i	i^{th} measured value of variable; x-value of i^{th} data pair
X_{new}	new value of X used in 1^{st}-order linear regression model
$Y(X_{new})$	1^{st}-order linear regression model
Y_i	y-value of i^{th} data pair

REPORT DOCUMENTATION PAGE

Form Approved
OMB No. 0704-0188

1. AGENCY USE ONLY (*Leave blank*)	2. REPORT DATE	3. REPORT TYPE AND DATES COVERED
	April 2004	Technical Memorandum

4. TITLE AND SUBTITLE

Performance of Thermal Mass Flow Meters in a Variable Gravitational Environment

5. FUNDING NUMBERS

WBS–22–101–52–02

6. AUTHOR(S)

John E. Brooker and Gary A. Ruff

7. PERFORMING ORGANIZATION NAME(S) AND ADDRESS(ES)

National Aeronautics and Space Administration
John H. Glenn Research Center at Lewis Field
Cleveland, Ohio 44135–3191

8. PERFORMING ORGANIZATION REPORT NUMBER

E–14482

9. SPONSORING/MONITORING AGENCY NAME(S) AND ADDRESS(ES)

National Aeronautics and Space Administration
Washington, DC 20546–0001

10. SPONSORING/MONITORING AGENCY REPORT NUMBER

NASA TM—2004-213045

11. SUPPLEMENTARY NOTES

Responsible person, John E. Brooker, organization code 6711, 216–433–6543.

12a. DISTRIBUTION/AVAILABILITY STATEMENT

Unclassified - Unlimited
Subject Category: 34 Distribution: Nonstandard

Available electronically at http://gltrs.grc.nasa.gov

This publication is available from the NASA Center for AeroSpace Information, 301–621–0390.

12b. DISTRIBUTION CODE

13. ABSTRACT ***(Maximum 200 words)***

The performance of five thermal mass flow meters, MKS Instruments 179A and 258C, Unit Instruments UFM-8100, Sierra Instruments 830L, and Hastings Instruments HFM-200, were tested on the KC-135 Reduced Gravity Aircraft in orthogonal, coparallel, and counterparallel orientations relative to gravity. Data was taken throughout the parabolic trajectory where the g-level varied from 0.01 to 1.8 times normal gravity. Each meter was calibrated in normal gravity in the orthogonal position prior to flight followed by ground testing at seven different flow conditions to establish a baseline operation. During the tests, the actual flow rate was measured independently using choked-flow orifices. Gravitational acceleration and attitude had a unique effect on the performance of each meter. All meters operated within acceptable limits at all gravity levels in the calibrated orthogonal position. However, when operated in other orientations, the deviations from the reference flow became substantial for several of the flow meters. Data analysis indicated that the greatest source of error was the effect of orientation, followed by the gravity level. This work emphasized that when operating thermal flow meters in a variable gravity environment, it is critical to orient the meter in the same direction relative to gravity in which it was calibrated. Unfortunately, there was no test in normal gravity that could predict the performance of a meter in reduced gravity. When operating in reduced gravity, all meters indicated within ±5 percent of the full scale reading at all flow conditions and orientations.

14. SUBJECT TERMS

Mass flow meters; Gravitational effects; Buoyancy; Heat transfer; Uncertainty analysis

15. NUMBER OF PAGES

27

16. PRICE CODE

17. SECURITY CLASSIFICATION OF REPORT	18. SECURITY CLASSIFICATION OF THIS PAGE	19. SECURITY CLASSIFICATION OF ABSTRACT	20. LIMITATION OF ABSTRACT
Unclassified	Unclassified	Unclassified	